Materials Science Forum
ISSN: 1662-9752, Vol. 1186, pp 97-107
doi:10.4028/p-6UdHbQ

Submitted: 2025-12-19
Revised: 2026-02-14
Accepted: 2026-02-25
Online: 2026-04-16

Impact of Separating Agents on the Deformation Regime in Aluminum Roll-Cladding Processes

Muhr Felix[1,a*], Höniger Benedikt[2,b], Niemietz Philipp[1,c], Frohn-Sörensen Peter[2,d], Engel Bernd[2,e] and Bergs Thomas[1,f]

[1]Manufacturing Technology Institute MTI of RWTH Aachen University, Campus-Boulevard 30, 52074 Aachen, Germany

[2]Forming Technology Siegen, Institute of Production Technologies, University of Siegen, Breite Straße 11, 57076 Siegen, Germany

[a*]f.muhr@mti.rwth-aachen.de, [b]benedikt.hoeniger@student.uni-siegen.de, [c]p.niemietz@mti.rwth-aachen.de, [d]peter.frohn@uni-siegen.de, [e]bernd.engel@uni-siegen.de, [f]t.bergs@mti.rwth-aachen.de

Keywords: partial roll-cladding, battery cooling, heat exchanger, e-mobility, BEV, aluminum.

Abstract. Application fields and requirements for roll-cladded cooling plates are continuously rising. Especially as part of the thermal management systems in battery electric vehicles (BEV), the share of roll-cladded cooling plates is growing. A deeper understanding of the deformation regime in the roll bite is needed to completely fulfill the high quality, performance and cost requirements of the automotive industry. Whereas most cause-effect relationships in the roll-cladding process have been scientifically evaluated, the influence of separating agents on the deformation regime in partial roll-cladding has not yet been investigated. To examine this relationship, an experimental set up is created and trials are conducted on a laboratory size roll-cladding mill. Two different aluminum alloy blanks are joined together under temperature by roll-cladding without the application of strip tensions and with different separating agent patterns. The results show: Firstly, there is a correlation between the materials' relative flow stress difference and their relative deformation. Secondly, the separating agents' areal share over the blank width significantly impacts the deformation regime in the roll bite. Thirdly, in areas with separating agent there is a correlation between the surface elongation of the bottom blank and the elongation of the contact interface between the blanks, which governs the later cooling channel tolerances. To use the results in the industrial application, the impact of so far neglected parameters such as strip tensions have to be considered in future research.

Introduction

Political and social awareness have led and will further lead to a significant increase in the worldwide share of produced BEV compared to the share of internal combustion engine vehicles (ICEV) [1]. To be able to participate in future market growth, it is crucial for the original equipment manufacturers (OEMs) and their supplier base to decrease the cost and increase the performance of BEV cars by using innovative solutions [2, 3]. Example given, the range of a BEV is nowadays on average significantly lower than the range of an ICEV. Additionally the BEV production costs are roughly 45% higher than the ICEV costs. [4] The resulting ever-rising customer demand for an improved range performance, cost and safety of BEV increases the importance of the battery and its thermal management system. Today's state-of-the-art lithium-ion batteries require a constant and homogenously distributed cell-temperature between 20 °C and 40 °C. Any negligence of this requirement can lead to safety risks, such as the self-ignition of the battery, or a significant reduction of the BEV's performance respectively it's lifespan. There are different types of battery cooling or heating technologies used in today's BEVs. One method is the indirect cooling by a cooling plate, that is placed either above, below or between the battery cells. A cooling fluid, flowing in channels, is extracting the heat from the cells. [5] The process of roll-cladding has been used for decades to produce similar evaporator plates in the household industry, e.g. in refrigerators. Nowadays, the first BEVs in series feature use roll-cladded cooling plates as part of the thermal management system. [6]

Compared to other technologies the use of cooling plates in BEVs is evaluated as generally suitable [7]. Alongside with the roll-cladding [8] there are different processes to produce cooling plates, such as the brazing technology [9]. This paper focusses on the partial roll-cladding process. Automotive requirements regarding cooling performance, geometry, permanent bonding of the layers and cost make it inevitable to deepen the understanding of the partial roll-cladding process for aluminum cooling plates.

State of the Art

To produce aluminum cooling plates, two sheets are joined together by rolling under pressure, temperature and surface area enlargement in the partial hot roll-cladding process. In the area of the later cooling channel pattern a separating agent is applied to locally avoid joining of the sheets. These areas are inflated in an internal high pressure forming process after roll-cladding and subsequently form the channels guiding the cooling fluid. [8] As only parts of the blanks are roll-cladded, the process is referred to as partial roll-cladding.

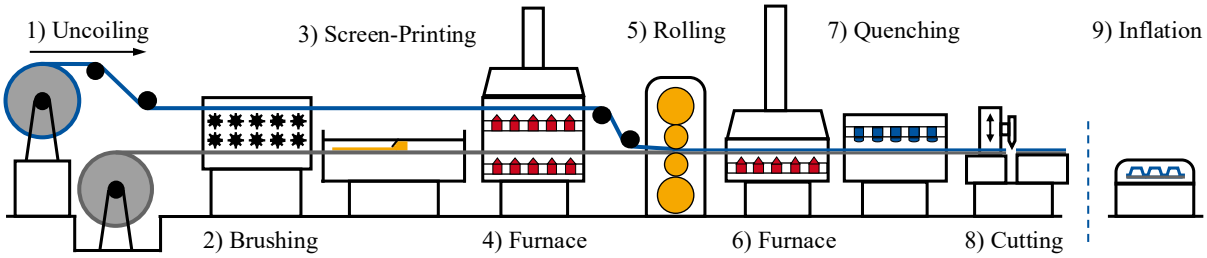

Fig. 1. Partial roll-cladding serial process for production of cooling plates.

Fig. 1 shows the serial process of continuous partial roll-cladding in an overview. Two strips are uncoiled (1) and brushed (2) on the bottom side of the top strip and on the top side of the bottom strip with steel brushes to remove oxides and generate a particular surface roughness supporting the subsequent mechanical and chemical joining mechanisms. Thereafter, a graphite separating agent is applied on the top side of the bottom strip with a screen-printing process (3) before both strips are heated in a furnace (4). In the roll bite the two brushed and heated strips are joined together under high forces (rolling force in combination with strip tension). Usually, a quarto rolling mill (5) with one pair of work rolls and one pair of backup rolls is used. To control the hardening effect occurring during the rolling process, the joined strip is heated again to recrystallize and then quenched with water to set the final material parameters (6). After cutting the blanks from the coil (7), the areas with separating agent are being inflated (9) in an internal high pressure forming process before they receive their final shape on a contour cutting press. Finally, the connecting points to the thermal management system of the vehicle's battery assembly are joined on the plate. For serial production continuous processes are often used, but partial roll-cladding of single blank packages is as well state-of-the-art. In that case, the preparation steps need to be performed separately and often in a manual process, however strip tensions cannot be applied.

Schmidtchen (2017) describes the bonding mechanisms governing the cladding process in three steps: Initially during the cladding process the roughened surfaces of the two strips are being further opened, which exposes metallically bare surfaces on both sides of the contact interface. These surfaces are not yet affected by oxides or other environmental interactions. Adsorption processes in the boundary surfaces initiate a first bonding before diffusion processes strengthen the bonding between the materials. One important parameter for technically reliable bonding is a pronounced thickness reduction of the materials. For cold roll-cladding the minimum thickness reduction/plastic deformation is defined at around 30-70%, whereas in hot roll-cladding a sufficient bond can already be created at thickness reductions/plastic deformations starting from 20%. [10]

Industrial practice shows that often thickness reductions higher than 20% are used in hot-roll-cladding to ensure sufficient bonding strength between the materials. Melzner and Hirt (2014) have observed that when using different material alloys, severe differences in thickness reduction can occur

during rolling, because the softer material is being deformed stronger than the harder material. They were able to show that a temperature difference between both incoming materials can compensate for this effect. [11] The effect of different reductions when using materials with different flow stresses (like aluminum and copper) was also described in Bauer and Schadt (2017), supporting the conclusion that the softer material has a higher reduction than the harder one. This leads to relative velocities and thus frictional stresses between the two cladding partners. An increase in the incoming materials' thickness difference increases the relative velocities between the cladding partners. [12] Melzner and Hirt (2017) stated that it is important for a strong bond that the relative velocities between the two materials during the cladding process are minimized, otherwise the bond can break up due to high shear stresses during rolling. Methods are described to minimize the difference in thickness reduction between the top and the bottom material by e.g. varying the roll-diameter, the incoming strip thicknesses and the flow stress differences between the materials. [13]

In contrast to the referenced literature, that focuses on the impact of temperature and roll bite geometry differences on the bonding quality, the focus of this paper lies on the influence of the separating agent on the elongation of the channel pattern. An impact on the deformation regime is expected. Considering the high level of the minimum required thickness reduction threshold, evidently even small reduction differences in the bottom blank can significantly change the geometry, especially the length variation, of the channel pattern applied on the bottom blank. For the battery cooling plate alongside the requirement of sufficient bonding, a homogeneous cooling performance is needed, which highlights the importance of correctly formed cooling channels.

In summary, significant research has been underwent on most process-influencing parameters regarding the complex, thermo-mechanically coupled process of roll-cladding. However, the influence of the separating agent and its areal shape on the complex deformation behavior in the roll bite is yet to be examined to fully utilize the technology's potential.

Materials and Methods

Experimental setup.

To investigate the influence of presence of separating agent on the thickness reduction of the cladding partners, a laboratory size quarto rolling mill (see Fig. 2 b)) is used at RWTH Aachen University. The maximum rolling force of the mill is $F_{max} = 2.800$ kN. Work rolls with a diameter of $D_{WR} = 150$ mm are used to roll-clad two materials in a blank size of $l_0 = 450$ mm length and $b_0 = 150$ mm width. For the top blank a soft EN-AW-1050-O and for the bottom blank a harder EN-AW-3003-H14 aluminum alloy is used. The blanks are manually cut to shape from coil material, straightened and brushed on the contact sides of both blanks. Subsequently, the separating agent is manually applied on the brushed surface of the bottom blank via screen printing technology. To ensure that both blanks are reproducibly aligned on top of each other, they are spot welded together over the width of the plate on one side. The incoming thickness of both blanks is $h_{0,top} = h_{0,bottom} = 2$ mm. To heat up the plates a chamber furnace (see Fig. 2 a)) is used in which both blanks are heated for 5 minutes at a furnace temperature of $T_{Furnace} = 430$ °C, before they are transported manually to the roll bite. A temperature difference of 30 °C during transport has been verified by contact temperature measurements. Consequently, the roll bite temperature is assumed as $T_{Rollbite} = 400$ °C. A total number of $n_{print} = 8$ blank packages are roll-cladded with a separating agent applied between the blanks, a reference amount of $n_{ref} = 3$ is rolled without separating agent as a control group. The targeted thickness reduction of the blank package is calculated to approximately -50% by (Eq. 1):

$$\varepsilon_{h,package,target} = \frac{h_1 - h_0}{h_0} * 100\,\% \approx -50\,\%. \quad (1)$$

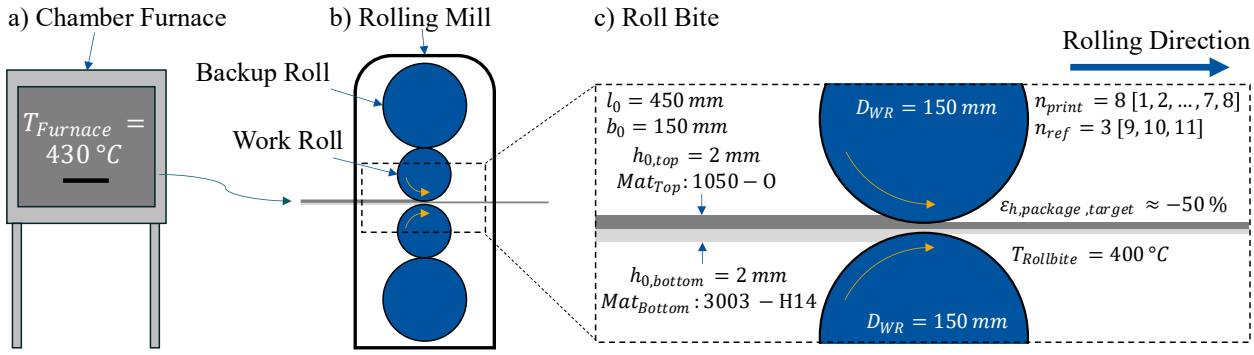

Fig. 2. Experimental setup for rolling trials with a) chamber furnace, b) laboratory size rolling mill and c) detail view of roll bite with process parameters and sample specifications.

To investigate not only the influence of the presence of separating agent, but also the influence of the areal share and shape, a special screenprint pattern, shown in Fig. 3 b), is introduced. To support a sufficiently homogenous deformation regime in the roll bite, the space between the different sectors is designed to be at least in the size of the contact length of roll and material. Based on Kopp and Wiegels (1999) this length is defined according to the elementary plasticity theory to approximately 12,5 mm by (Eq. 2) [14]:

$$l_d = \sqrt{\frac{D_{WR}}{2} * \Delta h} = \sqrt{\frac{D_{WR}}{2} * (h_{0,top} + h_{0,bottom} - h_{1,top} - h_{1,bottom})}. \quad (2)$$

Due to the time and distance needed to close the mill to the desired gap, there is extra space before sector A held up for the mill to close, highlighted in dark grey in Fig. 3. The same applies for the end of the plate. These front and rear trim sections are scrap and not used for evaluation. Between the dark grey areas different separating agent sectors are designed to represent different areal shares of separating agent, different symmetries and gradients. The areal share of the separating agent varies from 0 % in sector E to 100 % in sector F. In sector D, a short separating agent area is followed by a short, bonded area and a short separating area again to evaluate the influence of the length of the patterns. The pattern in sector C is the only asymmetrical pattern intended to create different elongations over the width of the blanks. Patterns in sectors B & A are geometries that are typically used in the automotive cooling plate industry. All sectors are the same length and width.

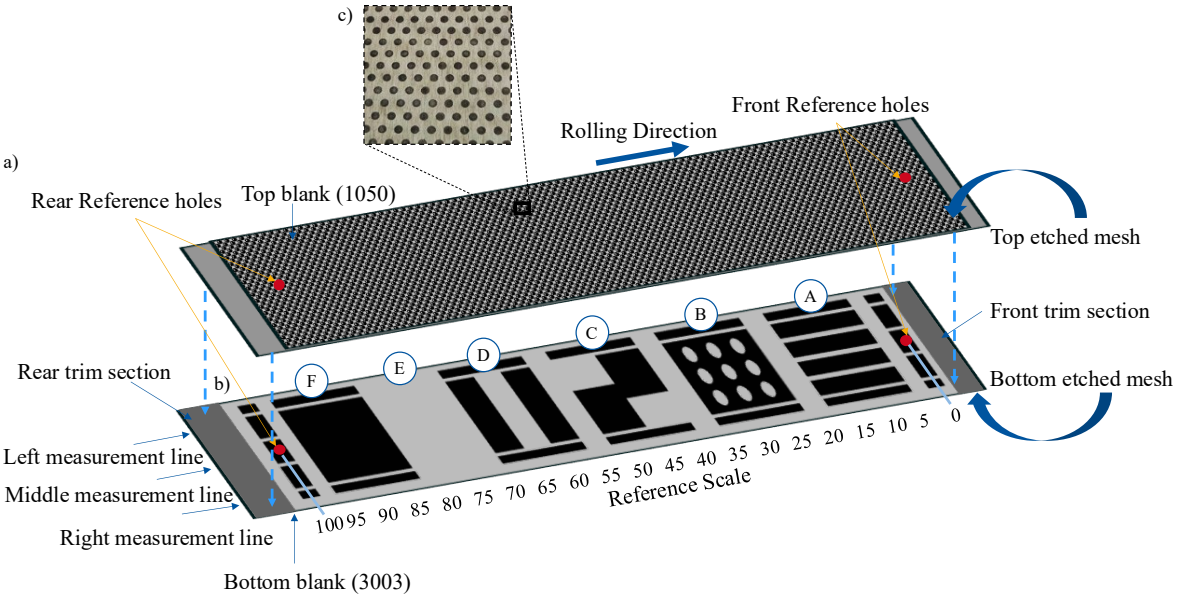

Fig. 3. a) Blank package before rolling with b) separating agent pattern (black) on bottom blank and c) etched mesh on outer surfaces.

The creation of the test pattern was based on the hypothesis that varying areal shares of separating agents over the rolling width must provoke alterations in the integral frictional force through altered local frictional behaviors in areas with and without separating agent. The share of separating agent over the width is determined in CAD in 1 mm steps and quantified by (Eq. 3):

$$x_{agent} = \frac{A_{agent}}{A_{total\_area}} * 100\ \%. \quad (3)$$

Evaluation method.

In this paper, etching of a raster pattern intended for optical strain evaluation is used to make the surface layer deformations of the top side of the top blank and the bottom side of the bottom blank visible. All 22 blanks ($(n_{print} + n_{ref}) * 2 = 22$) are manually etched on the outsides with a pattern, shown in Fig. 3 c), using an electrolyte DE20 from Östling Marking Systems. Because of the high deformations, the contrast of the points is not sufficient to allow a photo optical measurement of the deformations. For this reason, the distance of the points after rolling is measured with a caliper and set in relation to the distance before rolling. Additionally, reference holes are drilled through both blanks together prior to rolling to localize the start and end point of the separating agent pattern after rolling. The positions of the reference points are shown in Fig. 3.

Before and after the roll-cladding process, thickness measurements of all blanks by micrometer screw are conducted at 10 equidistant measuring points along the blank length with 30 mm space from each blank's edge. To evaluate the start and end point of the different separating agent sectors, a non-destructive thickness measurement technique is used, which is capable to detect the single layer thickness in areas with separating agent as well as the total thickness in areas without separating agent. At points where the thickness transitions from single to double layer, the start or end point of a sector is defined. These points are marked on the outer surface. The length of the sector is measured with a caliper afterwards and is set in relation to the sector length before rolling to determine the elongation of each pattern. This method is adapted from Kleiner et al. [15].

A significant difference in reduction and elongation of the top vs. the bottom blank is anticipated due to differences in the flow stresses. To align all measurements after rolling on the original separating agent pattern, a reference scale of 0 to 100 is defined between the two reference holes on both blanks, see Fig. 3. The distance between the reference holes after rolling is divided into 100 equisized segments for each blank. All further measurements are linked to these reference points rather than to the absolute position on the blank.

Experimental constraints lead to elongation deviations compared to the target elongation $\varepsilon_{h,package,target}$. The total thickness reduction of the blank packages i is defined as $\varepsilon_{h,package,i}$. A normalization factor is required to make the absolute thickness reductions between the blank packages comparable. The normalization factor for each blank package i is defined in (Eq. 4) as:

$$x_{norm,i} = \frac{\varepsilon_{h,package,target}}{\varepsilon_{h,package,i}}, \quad (4)$$

with the thickness reduction being defined in (Eq. 5) as:

$$\varepsilon_{h,package,i} = \frac{h_{1,i} - h_{0,i}}{h_{0,i}} * 100\ \%. \quad (5)$$

For the incoming thickness $h_{0,i}$ the sum of bottom and top blank incoming thickness (averaged over each blank) is considered. For $h_{1,i}$ the averaged sum of the total package outgoing thickness in areas without separating agent is considered. The total length elongation of each blank package is calculated as in (Eq. 6):

$$\varepsilon_{l,i} = \frac{l_{1,i} - l_{0,i}}{l_{0,i}} * 100\ \%, \quad (6)$$

As the blank width is assumed to be constant ($\varepsilon_b = 0$), the normalized elongation is obtained according to (Eq. 7):

$$\varepsilon_{l,norm,i} = \frac{l_{1,i} - l_{0,i}}{l_{0,i}} * x_{norm,i} * 100\ \%. \quad (7)$$

For each blank the normalized elongation is calculated in (Eq. 8) and (Eq. 9) as:

$$\varepsilon_{l,top,i} = \frac{l_{1,top,i} - l_{0,top,i}}{l_{0,top,i}} * x_{norm,i} * 100\ \%, \quad (8)$$

$$\varepsilon_{l,bottom,i} = \frac{l_{1,bottom,i} - l_{0,bottom,i}}{l_{0,bottom,i}} * x_{norm,i} * 100\ \%. \quad (9)$$

If e.g. $\varepsilon_{l,top,i} = 100\ \%$ the strip length has been doubled during the rolling process. The length l_l is either taken from the distance measurement between the etched mesh or the distance between start and end of a separating agent sector. The above-mentioned formulas are based on Kopp and Wiegels (1999). [14]

Results and Discussion

During the experiment it was observed that all 11 plates had a saber like deformation in the direction of rolling as shown in Fig. 4, meaning that the blank edges formed a curve instead of a linear elongation. This can be explained by slightly different roll gap settings along the width causing one side to be elongated more than the other side. Another reason for the saber is that the blanks were rolled without strip tensions supporting a straight strip control.

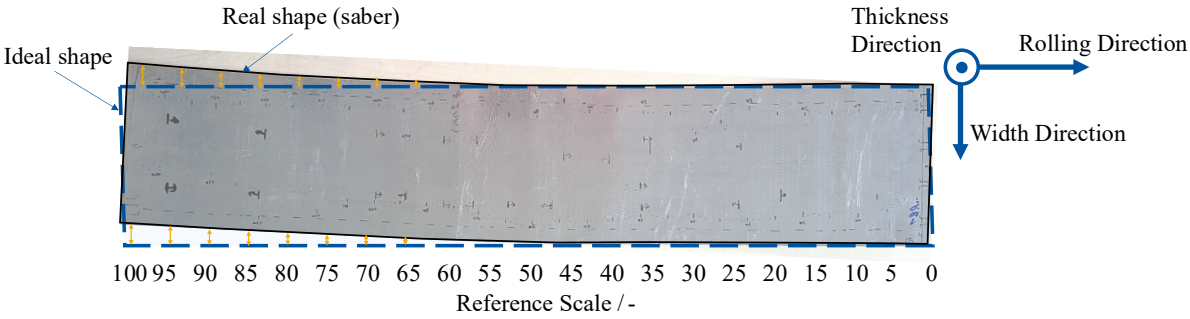

Fig. 4. Comparison of ideal with real sample shape after rolling.

Total elongation difference test pattern vs. reference samples.

Fig. 5 shows the total normalized elongation separately for the bottom and top blank surface based on the length difference of the etched points from reference point 0 to 100 (see chapter evaluation method). Fig. 5 a) shows the results of group n_{print} with separating agent whereas Fig. 5 b) shows results for the reference group n_{ref} without separating agent. As anticipated, because of flow stress differences in both cases the surface of the harder bottom material (EN-AW-3003-H14) always elongates less than the surface of the softer top material (EN-AW-1050-0). If separating agent is present between the blanks it can be stated that the bottom material elongates even less than in the case where no separating agent is present. The surface of the bottom material sees an elongation of roughly 85 % with separating agent (left box in Fig. 5 a)) and roughly 97 % without separating agent (left box in Fig. 5 b)). The surface of the softer top blank material on the other hand elongates more (roughly 138 %) when separating agent is present (right box in Fig. 5 a)) and less (roughly 123 %) when no separating agent is present (right box in Fig. 5 b)). The observed result is the inverse for the two materials. The effect that the top blank generally elongates more than the bottom blank can also be seen in Fig. 5 a) and b). It is visible in Fig. 5 c) that the top material is always longer than the bottom material.

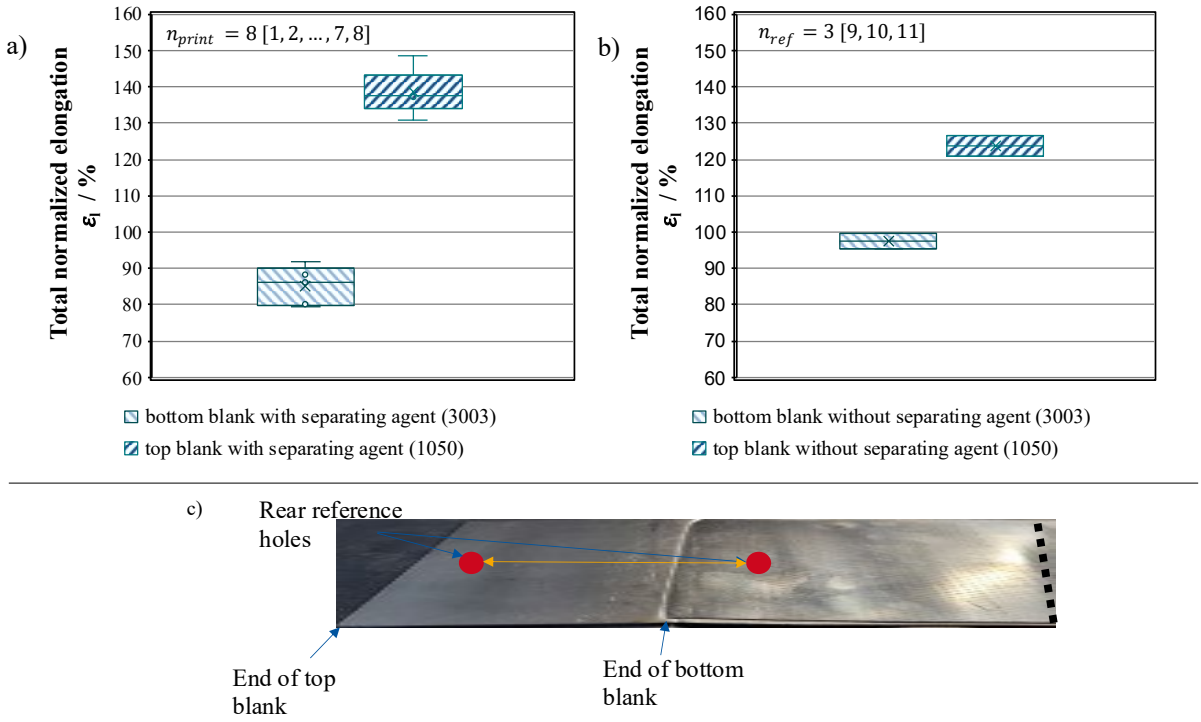

Fig. 5. a) Total normalized elongation of top and bottom blank with and b) without separating agent and c) example for elongation differences between top and bottom blank at rear trim section.

Local elongation difference top vs. bottom material.

Analyzing the local normalized surface elongations in reference to the separating agent pattern, the above-mentioned phenomenon is confirmed. Fig. 6 shows the local normalized surface elongation of both top (orange, full line) and bottom (blue, dashed line) blank referenced on the separating agent pattern. It is qualitatively visible that in areas where separating agent is present, the hard bottom material elongates less, and the soft top material elongates more. In the areas without separating agent the inverse is visible. In addition, evidently in sector E both elongations differ by just roughly 17 %-points while in sector F the elongations are, at maximum, nearly 106 %-points apart from each other. The standard deviation of each measurement is indicated by vertical error bars where the highest standard deviation is observed in sector F. In addition to that, the elongation is more pronounced for the top material in sector F, which is correlated to the observed saber-like edge deformation. A thickness measurement has been conducted to support the theory of the influence the separating agent has on the deformation.

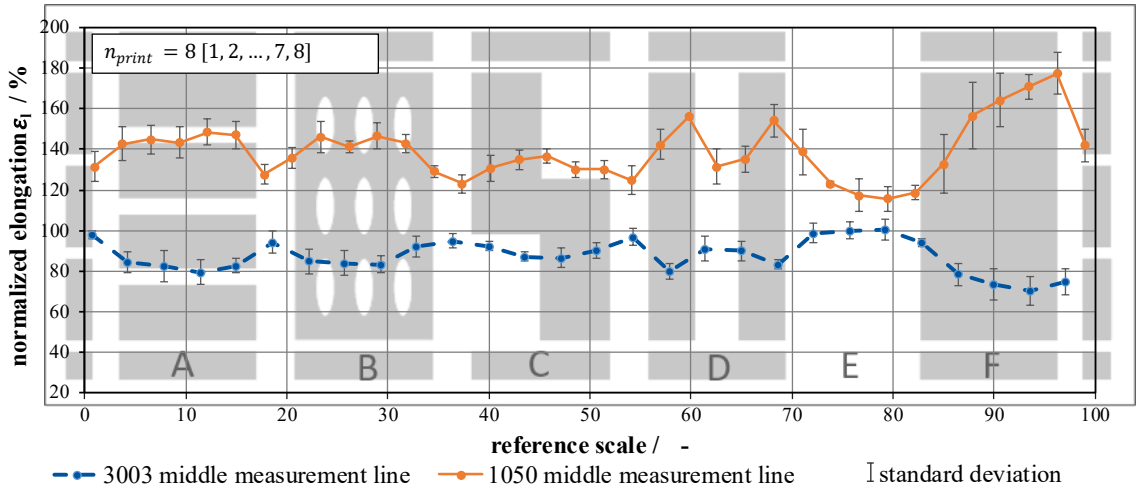

Fig. 6. Local elongation of bottom (3003) and top (1050) blanks with separating agent on middle measurement line.

Local elongation difference in asymmetrical separating agent areas.

Contrary to Fig. 6, Fig. 7 shows the normalized elongation only of the harder bottom material. The dashed blue line shows the elongation on the left and the full blue line the elongation on the right side. It can be stated that both have the same qualitative progression. There are two areas that need to be highlighted though. One is sector C, the other one is sector F. In sector C (see Fig. 7 b)), which is the only asymmetrical separating agent area of the screenprint, it is visible that when there is more separating agent on the left compared to the right side, the first-mentioned is elongated less. If there is more separating agent on the right side than on the left side, the effect switches to the opposite. This again proves the above discovered observation. In sector F the left side is elongated less than the right side, which agrees to the observed saber phenomenon.

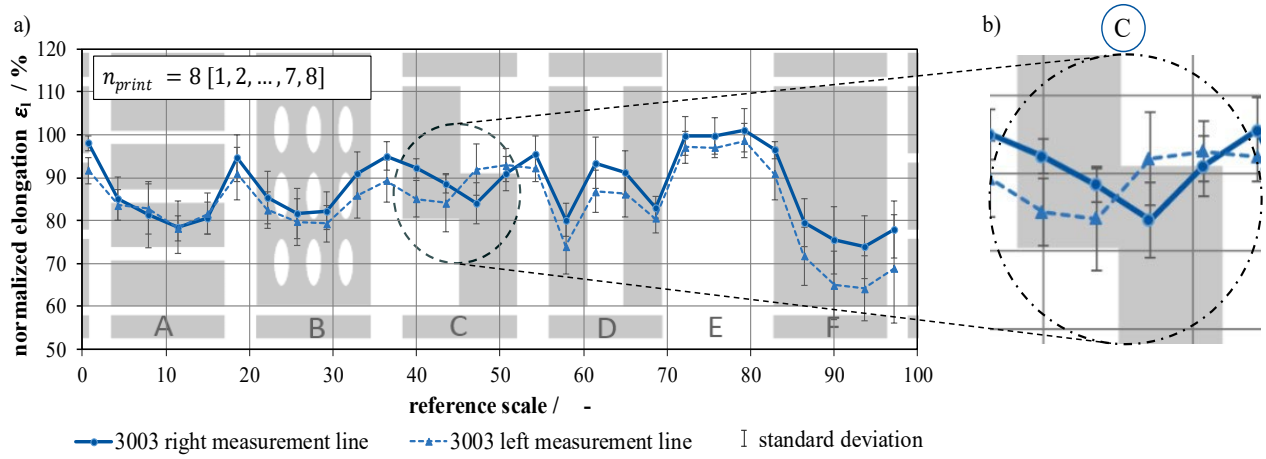

Fig. 7. a) Local elongation of left and right measurement line of bottom (3003) blank and b) detail view sector C.

Correlation between separating agent areal share and elongation.

In Fig. 8 the normalized elongation on the middle measurement line over the areal share of separating agent over the width is plotted separately for the bottom and the top blank. The dashed blue line shows a linear regression curve fitting the points. It is visible that for the bottom material there is a strong negative correlation between elongation and share of separating agent, whereas for the top blank there is a positive correlation. This fits the above-mentioned results, underlining that the higher the share of separating agent over the width gets, the smaller the elongation gets for the hard bottom and the higher it gets for the soft top material.

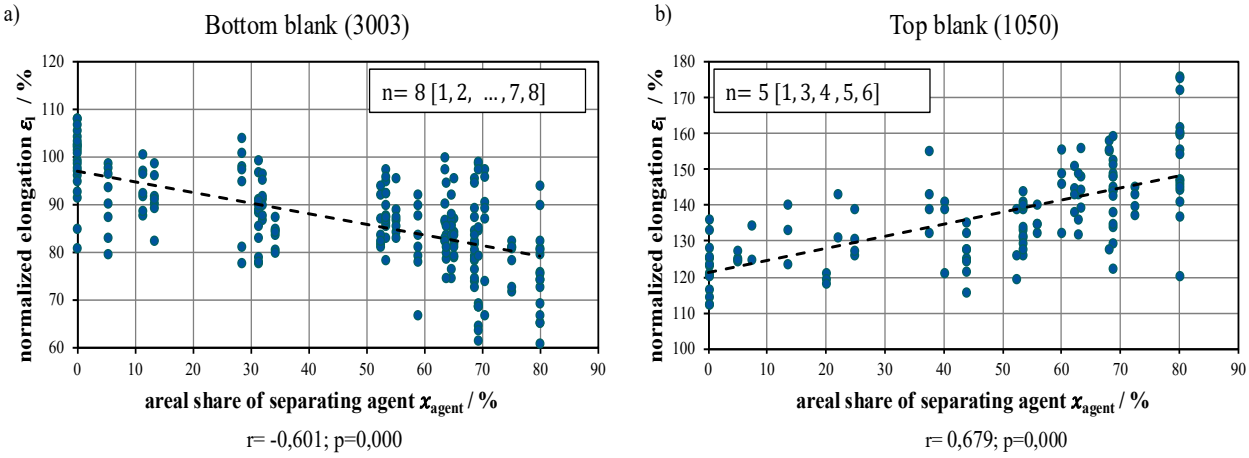

Fig. 8. Correlation between separating agent areal share and a) bottom blank (3003) surface elongation and b) top blank (1050) surface elongation.

Correlation of surface elongation and elongation of contact area between blanks.

Up to now, the focus of this paper was to evaluate the surface elongation of the outside surfaces of the blank package. For the application of the roll-cladding technology in the BEV-industry, however, it is of high importance how the separating pattern is being elongated in the interface between the two blanks, as this governs the later geometrical tolerances of the cooling channel pattern. In this chapter the elongation of the pattern is evaluated by locating the start and end point of each pattern and measuring the elongated distance (see chapter evaluation method). Fig. 9 shows the averaged normalized elongations between the outer surface of the bottom (blue) and surface of the top material (red) as well as the contact area (grey) elongation between top and bottom blank. In the fully bonded area (sector E) it is visible that the surface of the hard bottom material is elongated by 97 %, the contact area is elongated by 107 % and the surface of the soft top material is elongated by 123 %. The bond between the materials in the contact area explains this gradient. In sector F, where separating agent is applied, evidently the contact area is elongated in the same way as the surface of the hard bottom material by 62 % whereas the soft top material is elongated by 168 %. Thus, it is concluded that the elongation of the separating agent area in sector F can be derived from the surface elongation of the harder bottom blank material.

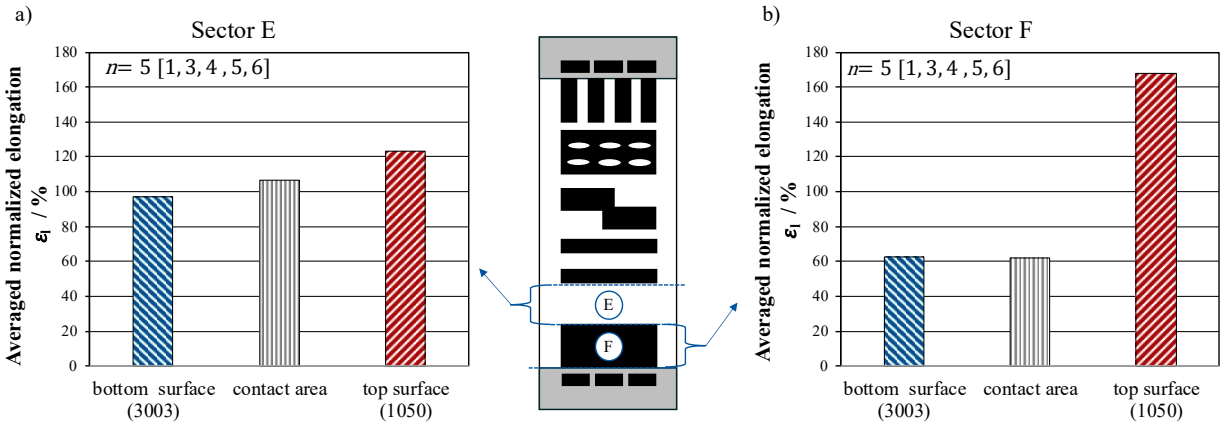

Fig. 9. Elongation of bottom blank surface (3003), contact area and top blank surface (1050) in a) sector E and b) sector F.

Restrictions of investigation.

The experiments have been conducted on a laboratory size rolling mill in a discontinuous process and without application of strip tensions. This will presumably have a strong impact on the deformation regime. The roll diameters were by factor 2.5 smaller than in a serial production line. Taking Melzner and Hirt (2017) into consideration it can be expected that the roll diameter has a high influence on the different elongations of the top and the bottom blank [13]. The measuring methods used were partially manual. Despite best possible diligence, deviations in repeatability cannot be completely ruled out. In particular visually difficult to identify areas on some of the etched grids had to be detected manually. Finally, the elongations were only measured in three layers, which are the outer surface of the top blank, the interface area and the outer surface of the bottom blank. With the current experimental set up it is not possible to fully visualize the deformations that occur between these layers, whereas validated simulation models might provide valuable insights.

Summary and Outlook

The present paper focused on the influence of a separating agent on the deformation regime in the roll gap of a roll-cladding process of EN-AW-3003-H14 and EN-AW-1050-O. The focus lied on the elongation of different separating agent patterns as this is decisive for the cooling channels tolerances of cooling plates that are produced with this process and used in battery electric vehicles. Under the defined experimental conditions, three main conclusions are drawn:

1. The materials' relative deformation in the roll bite correlates with its relative flow stress: The softer material tends to be elongated more, because the flow stress is approximately 40 % lower than the flow stress of the harder material at 400 °C at the given deformation (see Fig. 5, 6 and 9).
2. The harder material roughly elongates 36% less when separating agent is applied (sector E vs. sector F), whereas the softer material roughly elongates 36% more when separating agent is applied (sector E vs. sector F) (see Fig. 9). This not only has an impact on the final cooling channel pattern geometry, but can also increase relative movements between the layers, resulting in inner stress or in the worst case in a delamination of the bond that could have fatal consequences (see Fig. 5-9).
3. The surface elongation of the harder bottom material represents the elongation of the contact interface between both materials if separating agent is applied with a decent accuracy. If no separating agent is applied, a deviation is observed. This is an important finding since the elongation of the interface is hard to measure directly and determines the geometrical tolerances of the later cooling channel pattern of the cooling plate (see Fig. 9).

Table 1 shows the qualitative relations of the thickness as well as the thickness reduction comparing areas with separating agent to areas without separating agent.

Table 1. Qualitative relations of thickness, thickness reduction and elongation of bottom (3003) and top (1050) blank with and without separating agent.

		with separating agent		**without** separating agent
Thickness	Bottom blank	Thickness +	⟷	Thickness -
	Top blank	Thickness -	⟷	Thickness +
Thickness Reduction	Bottom blank	Thickness Reduction -	⟷	Thickness Reduction +
	Top blank	Thickness Reduction +	⟷	Thickness Reduction -
Elongation	Bottom blank	Elongation -	⟷	Elongation +
	Top blank	Elongation +	⟷	Elongation -

Future research should continue to investigate the influence of the separating agent layer on the deformation regime in the roll bite. Especially, it is important to conduct further experiments under conditions closer to serial production and not on a laboratory size mill. The application of strip tension and larger work roll diameters will have an influence on the relationships described. Furthermore, it is important to set up a simulation model to deepen the understanding of the local deformation governing the pass through of the roll bite. Current simulation and AI methods, if trained with real production data, can open new possibilities in process development and should be used in further research [16].

References

[1] D. Harrison and C. Ludwig, "Electric Vehicle Battery Supply Chain Analysis: How Battery Demand and Production are Reshaping the Automotive Industry," ABB Technik, 2021.

[2] Martin Wietschel et al., "Batterien für Elektroautos: Faktencheck und Handlungsbedarf – Ein Update (Policy Brief 01 / 2025)," 2025.

[3] A. Kampker and H. H. Heimes, Eds., Elektromobilität: Grundlagen einer Fortschrittstechnologie, 3rd ed. Berlin, Heidelberg: Springer Berlin Heidelberg, 2024. [Online]. Available: https://nbn-resolving.org/urn:nbn:de:bsz:31-epflicht-3052149.

[4] A. König, L. Nicoletti, D. Schröder, S. Wolff, A. Waclaw, and M. Lienkamp, "An Overview of Parameter and Cost for Battery Electric Vehicles," WEVJ, vol. 12, 2021, doi: 10.3390/wevj12010021.

[5] R. Korthauer, Ed., Handbuch Lithium-Ionen-Batterien, 1st ed. Berlin Heidelberg: Springer Berlin Heidelberg; Imprint: Springer Vieweg, 2013.

[6] L. Deng, Y. Li, P. Xu, Z. Chen, W. Zhou, and B. Li, "Fabrication and thermal performance of a novel roll-bond flat thermosyphon," Applied Thermal Engineering, vol. 181, 2020, doi: 10.1016/j.applthermaleng.2020.115959.

[7] S. Arora, "Selection of thermal management system for modular battery packs of electric vehicles: A review of existing and emerging technologies," Journal of Power Sources, vol. 400, pp. 621–640, 2018, doi: 10.1016/j.jpowsour.2018.08.020.

[8] S. Kasuba, "Aluminium roll bond - A single innovatie circuit for air conditioner, car radiator, refigerator and water heater," International Journal & Magazine of Engineering, Technology, Management and Research, vol. 1, S. 11–16, 2014.

[9] O. Arsenyeva, L. Tovazhnyanskyy, P. Kapustenko, J. J. Klemeš, and P. S. Varbanov, "Review of Developments in Plate Heat Exchanger Heat Transfer Enhancement for Single-Phase Applications in Process Industries," Energies, vol. 16, no. 13, 2023, doi: 10.3390/en16134976.

[10] M. Schmidtchen, "Mehrskalige Modellierung des Walzplattierens und des Walzens von Werkstoffverbunden," Habilitationsschrift, Fakultät für Werkstoffwissenschaften und Technologie, Technische Universität Bergakademie Freiberg, Freiberg, 2017.

[11] A. Melzner and G. Hirt, "Roll Bonding of Two Materials Using Temperature to Compensate the Material Strength Difference," AMR, 966-967, pp. 471–480, 2014, doi: 10.4028/www.scientific.net/AMR.966-967.471.

[12] H. G. Bauer and W. Schadt, Walzen von Flachprodukten, 1st ed. Berlin, Heidelberg: Springer, 2017. [Online]. Available: http://web.archive.org/web/20170518150321/http://werkstoffwoche.de/fileadmin/user_upload/69910_0_V11_Call_17_Walzen.pdf.

[13] A. Melzner and G. Hirt, "Investigations on the elongation differences of aluminum in two layer roll bonding," 2017, doi: 10.1063/1.5008228.

[14] R. Kopp and H. Wiegels, Einführung in die Umformtechnik, 1st ed. Aachen: Verlag Mainz, 1999.

[15] M. Kleiner et al., "Fertigung innovativer IHU-Stahlbauteile auf Basis neuartiger, partiell plattierter Blechhalbzeuge: Forschungsbericht P 565," 2006.

[16] M. Liewald et al., "Perspectives on data-driven models and its potentials in metal forming and blanking technologies," Prod. Eng. Res. Devel., vol. 16, pp. 607–625, 2022, doi: 10.1007/s11740-022-01115-0.

The publication of this article was funded by the RWTH Aachen University 10.13039/501100007210